Chapter 5

Seasonal Variations

5.1 Introduction

The second natural phenomenon about which MACRO can make a positive measurement is the seasonal variation in the absolute muon rate[1]. Although it is of meteorological rather then astronomical origin, the measurement of this phenomenon, demonstrates that MACRO is sensitive to small signals.

The variations in question arise due to seasonal temperature changes in the upper atmosphere at the altitudes where cosmic ray induced pions are born. This effect has been known since early in the history of cosmic ray physics[2,3,4,5]. These muons are the decay products of π and K mesons created in the high energy collisions between primary cosmic rays and nuclei from the atmosphere[6].

While this effect has been well studied by above ground cosmic ray experiments[7], underground measurements have been fewer and often not in agreement with theory[8,9,10,11,12,13,14,15,16,17]. MACRO is well suited to make this measurement, due to its depth and large area. The large area allows collection of high muon statistics even at the reduced rate of a large depth underground experiment. MACRO's depth of 3800 mwe is deeper than all the experiments referenced above and translates directly into a high energy threshold on the muons it can observe. This enhances the seasonal variation effect in two ways. First, the muons are too energetic to be likely

to decay before being observed. Second, at higher energies the mesons produced in the shower are dominated by interactions rather than decays, allowing a more direct probe of this seasonal effect. This analysis uses muons collected during the years 1991 to 1994 to search for this variation in rate as a function of season.

5.2 Meteorological effects on the Underground Muon Rate

The relation between muon intensity variations and atmospheric temperature has been expressed as[2]

$$\frac{\Delta I_\mu}{I_\mu^0} = \int_0^\infty dX \alpha(X) \frac{\Delta T(X)}{T(X)} \ , \qquad \textbf{(1)}$$

where $I_\mu = I_\mu(>E_{th})$ is the differential muon intensity integrated from the detector threshold E_{th} (≈1.2 TeV for MACRO, see Equation 4) to infinity, ΔI_μ are fluctuations about I_μ^0; $\alpha(X)$ is the "temperature coefficient" that relates the fluctuations in the temperature at atmospheric depth X, $\Delta T(X)/T(X)$, to the intensity fluctuations; and the integral is over atmospheric depth from the altitude of muon production (≈20 km, essentially infinity in our exponential atmosphere) to the ground. Depth X is in units of surface mass density, gm/cm^2.

Qualitatively, this relation is due to the density of the air in this column changing with temperature. As the temperature increases, the density decreases. At a lower density, the muon's parent mesons have a better chance to decay (producing a muon) rather than interacting (producing a lower energy cascade). Thus, the rate of

observable muons increases with temperature. There is also a variation in the rate caused by changes in the pressure, but that has been shown to be at least an order of magnitude smaller for the high energy interactions[7] which result in muons at MACRO. Therefore, the pressure effect has been neglected in this analysis.

5.2.1 The Derivation of the Temperature Coefficient

To find the proper quantitative form for Equation 1, we start with the differential intensity of muons as a function of energy at the surface of the Earth, as described by Gaisser[6]. This is dI_μ/dE_μ, and is found by integrating the production spectrum of muons P_μ over atmospheric depth X:

$$\begin{aligned}\frac{dI_\mu}{dE_\mu} &= \int_0^\infty dX\, P_\mu(X,E_\mu) \\ &= A \times E_\mu^{-(\gamma+1)} \times \left(\frac{1}{1+\frac{1.1E_\mu \cos\theta}{\epsilon_\pi}} + \frac{0.054}{1+\frac{1.1E_\mu \cos\theta}{\epsilon_K}} \right).\end{aligned} \qquad \textbf{(2)}$$

In this equation, E_μ is the muon energy; θ is the muon zenith angle; $\gamma = 1.78$ is the spectral index for the muons observed by MACRO[19]; and $\epsilon_\pi = 115$ GeV and $\epsilon_K = 850$ GeV are the pion and kaon critical energies (see Equation 26). As discussed by Ambrosio et al[19], the differential energy spectrum at MACRO is well matched by this expression.

However, MACRO cannot distinguish energies in its muon sample. It simply records all muons with enough energy to make it to MACRO through the rock overburden. Thus, a useful expression is the integral spectrum

$$I_\mu(>E_{th}) = \int_{E_{th}}^{\infty} dE_\mu \frac{dI_\mu}{dE_\mu} , \tag{3}$$

where

$$E_{th} = E_{th}(\theta,\phi) = 0.53\left(e^{0.4D} - 1\right) \tag{4}$$

for muons arriving at MACRO from direction (θ,ϕ), with E_{th} in TeV for rock depth D in km of water equivalent.

From Gaisser[6] and in analogy with Barrett[2], a fair approximation of the integral in Equation 3 that interpolates between high and low energy approximations is given by

$$I_\mu \approx B \times E_{th}^{-\gamma} \times \left[\frac{1}{\gamma + \frac{(\gamma+1)1.1E_{th}\cos\theta}{\epsilon_\pi}} + \frac{0.054}{\gamma + \frac{(\gamma+)1.1E_{th}\cos\theta}{\epsilon_K}} \right]. \tag{5}$$

To find the variation of the integral intensity one obtains by substituting Equation 2 into Equation 3, the pion production term P_μ must be expanded.

$$\begin{aligned} P_\mu(X,E_\mu,T_0+\Delta T) &= P_\mu(X,E_\mu,T_0) + (\partial P_\mu/\partial T)_{T_0}\Delta T(X) \\ &= P_\mu^0(X,E_\mu) + \eta^0(X,E_\mu)\Delta T(X) , \end{aligned} \tag{6}$$

where the superscript "0" denotes the evaluation of the temperature dependent functions at some given $T = T_0$. The expanded integral becomes

$$\begin{aligned} I_\mu(>E_{th},T_0+\Delta T) &= \int_{E_{th}}^{\infty} dE_\mu \int_0^{\infty} dX[P_\mu^0(X,E_\mu)+\eta^0(X,E_\mu)\Delta T(X)] \\ &= I_\mu^0 + \int_0^{\infty} dX \Delta T(X) \int_{E_{th}}^{\infty} dE_\mu \eta^0(X,E_\mu) \ , \end{aligned} \tag{7}$$

where $I_\mu^0 = I_\mu^0(>E_{th})$. By setting $\Delta I_\mu = I_\mu(T_0+\Delta T)-I_\mu^0$, the dependence of the muon intensity variations on the atmospheric temperature fluctuations ΔT can now be expressed in the usual way[2,7,17],

$$\frac{\Delta I_\mu}{I_\mu^0} = \int_0^{\infty} dX \alpha(X) \frac{\Delta T(X)}{T(X)} \ , \tag{8}$$

where the positive correlation between intensity and temperature changes, α, is given by

$$\alpha(X) = \frac{T(X)}{I_\mu^0} \int_{E_{th}}^{\infty} dE_\mu \eta^0(X,E_\mu). \tag{9}$$

The "negative temperature correlation" mentioned in the older references describes the decay of muons into electrons. It is not important for muons of the energy observable by MACRO[2], due to the time dilation experienced by these extremely relativistic muons.

5.2.2 **The Temperature Coefficient as Seen by MACRO**

For MACRO, the intensity is calculated by counting the muons over time,

$$I_\mu = \frac{N_i/t_i}{\epsilon A_{eff}\Omega} \ , \qquad \textbf{(10)}$$

where N_i are the single muons observed in time t_i, ε is the efficiency with which muons are detected and reconstructed in MACRO, A_{eff} is MACRO's effective area, and Ω the solid angle seen by the detector. A_{eff} and Ω remain constant for a given detector configuration. Since the intensity fluctuations are expected to be only a few percent in magnitude, care must be taken that the other variable in this equation, ϵ, also does not fluctuate and mask any interesting changes in the muon rate. To prevent this, a small subset of MACRO's muon data was selected consisting only of muon tracks for which the reconstruction efficiency has been shown to be unity (as described in Section 5.4). This data selection allows the calculation of a ΔI which is free from instrumental fluctuations. The intensity fluctuation calculation then becomes

$$\begin{aligned} \frac{\Delta I_\mu}{I_\mu} &= \left[\frac{\Delta N_i/t_i}{\epsilon A_{eff}\Omega}\right] \Big/ \left[\frac{N_i/t_i}{\epsilon A_{eff}\Omega}\right] = \frac{[\Delta N_i/t_i]}{[N_i/t_i]} \\ &= \frac{\Delta R_\mu}{\bar{R}_\mu} \approx \frac{(R_\mu - \bar{R}_\mu)}{\bar{R}_\mu} \ , \end{aligned} \qquad \textbf{(11)}$$

where $R_\mu = N_i/t_i$ is the muon rate MACRO observed during time t_i and $\overline{R} = \Sigma N_i/\Sigma t_i$ is the average rate of observed muons over the whole observing period Σt_i.

As discussed in Section 5.3, the definition of an effective temperature T_{eff} allows simplification of the integral in Equation 1,

$$\int_0^\infty dX\alpha(X)\frac{\Delta T_{eff}}{T_{eff}} = \alpha_T\frac{\Delta T_{eff}}{\bar{T}_{eff}} \approx \alpha_T\frac{(T_{eff}-\bar{T}_{eff})}{\bar{T}_{eff}}, \quad \textbf{(12)}$$

where α_T is the depth weighted temperature coefficient, and $\overline{T}_{eff}$ is the average effective temperature over the period Σt_i. Combining Equations 11 and 12, Equation 1 becomes

$$\frac{\Delta R_\mu}{\bar{R}_\mu} = \alpha_T\frac{\Delta T_{eff}}{\bar{T}_{eff}}, \quad \textbf{(13)}$$

where $\Delta T_{eff} = T_{eff}/\overline{T}_{eff}$. This is the equation used to extract α_T from MACRO's data in this analysis.

5.3 The Effective Temperature

The "Effective Temperature" is an approximation that allows the atmosphere to be treated as an isothermal body. In reality, temperature varies considerably with atmospheric depth. However, a weighted average of the temperatures at various depths can be created. If the weights used in these averages are chosen properly, the average thus computed can be treated as the effective temperature of an isothermal atmosphere.

To choose these weights properly, we proceed from Equation 9, and integrate it over the whole atmosphere.

$$\alpha_T = \frac{T_{eff}}{I_\mu^0} \int_0^\infty dX \int_{E_{th}}^\infty dE_\mu \eta^0(X,E_\mu) \ . \qquad \textbf{(14)}$$

Here, α has become α_T, the "effective temperature coefficient", because we have assumed an isothermal atmosphere to bring $T(X)$ outside the integral over X to become T_{eff}, the effective isothermal temperature. Following Barrett's lead[2], T_{eff} is cast in the form

$$T_{eff} = \frac{\int_0^\infty dX T(X) \int_{E_{th}}^\infty dE_\mu \eta^0(X,E_\mu)}{\int_0^\infty dX \int_{E_{th}}^\infty dE_\mu \eta^0(X,E_\mu)} \ . \qquad \textbf{(15)}$$

This integral is difficult to evaluate. However, in the scaling limit, the X dependence of the pion production spectrum P_μ from Equation 6 can be factored[6],

$$P_\mu(X,E_\mu,T) = h(X) \Pi(E_\mu,T) \ . \qquad \textbf{(16)}$$

The scaling limit is the energy limit in which nuclei can be treated as collections of independent quarks for the purposes of collision cross sections. The scaling limit is valid for meson energies much greater than their critical energy[6]. MACRO's E_{th} of 1.2 TeV for muons leads to a minimum meson energy of 1.5 TeV from kinematics. Thus, the scaling limit is valid for pions (ϵ_π = 115 GeV) but not for kaons (ϵ_K = 850 GeV). To be able to factor P_μ into h and Π, the assumption must be made at

this point that MACRO's muons come solely from pion parents. The validity of this assumption is discussed in Section 5.9.

Taking advantage of this factoring, η^0 as introduced in Equation 6 becomes

$$\eta^0(X) = h(X)\left(\frac{\partial \Pi}{\partial T}\right)_{T_0}, \tag{17}$$

and Equation 15 becomes

$$T_{eff} = \frac{\int_0^\infty dX h(X) T(X)}{\int_0^\infty dX h(X)}. \tag{18}$$

The explicit expression for $h(X)$ in this limit is[6]

$$h(X) = \frac{\Lambda}{X}\left[e^{(-X/\Lambda_\pi)} - e^{(-X/\Lambda_N)}\right], \tag{19}$$

where $\Lambda = \Lambda_\pi\Lambda_N/(\Lambda_\pi - \Lambda_N)$; Λ_π = 160 gm/cm^2 is the atmospheric attenuation length for pions; and Λ_N = 120 gm/cm^2 is the atmospheric attenuation length for nucleons. Substituting Equation 19 into Equation 18 results in

$$T_{eff} = \frac{\int \frac{dX}{X} T(X)\left(e^{\frac{-X}{\Lambda_\pi}} - e^{\frac{-X}{\Lambda_N}}\right)}{\int \frac{dX}{X}\left(e^{\frac{-X}{\Lambda_\pi}} - e^{\frac{-X}{\Lambda_N}}\right)}. \tag{20}$$

Changing the integrals into sums, due to the discrete nature (there are eight measured temperature levels) of the temperature sampling in this analysis, produces the form used to calculate T_{eff} for this analysis,

$$T_{eff} \approx \frac{\sum_{i=1}^{8} \frac{T(X_i)}{X_i}\left(e^{\frac{-X_i}{\Lambda_\pi}} - e^{\frac{-X_i}{\Lambda_N}}\right)}{\sum_{i=1}^{8} \frac{1}{X_i}\left(e^{\frac{-X_i}{\Lambda_\pi}} - e^{\frac{-X_i}{\Lambda_N}}\right)} \; . \tag{21}$$

Checking Equation 20 by substituting it and Equation 17 back into Equation 14 reduces it to the expected

$$\begin{aligned} \alpha_T &= \frac{T_{eff}}{I_\mu^0} \times \int_0^\infty dX h(X) \times \int_{E_{th}}^\infty dE_\mu \frac{\partial \Pi}{\partial T} \\ &= \frac{T_{eff}}{I_\mu^0} \frac{\partial I_\mu}{\partial T} \; . \end{aligned} \tag{22}$$

5.4 The Muon Data

The muon data used in this analysis are a subset of the data discussed in Chapter 3. Only data from the years 1991 through 1994 were used, as that is the only time six SM of MACRO operated for which the needed upper atmosphere temperature data were available. To keep the detector configuration identical throughout this time

period (thus validating the claim of constant A_{eff} and Ω in Equation 10), only the lower half of MACRO was used for the track reconstruction, even though attico data was available for most of 1994. For the same reason, only data runs where all six supermodules were active were kept.

To ensure the assumption of unity ϵ is also valid, tight cuts were placed upon the events allowed into this analysis. Only single muons that crossed all ten planes of a single module were accepted. Multiple muons were disallowed to avoid any efficiency uncertainties. The requirement that a track stays within a single module avoids miscalculation of the overall streamer tube efficiencies caused by a module-crossing muon passing through the inter-module gaps rather than active detector volume. The ten plane requirement is the heart of these data cuts. Both calculation and the hand-scanning of many events have shown that for a muon which crosses ten active planes of streamer tubes, the track reconstruction efficiency is essentially 100%.

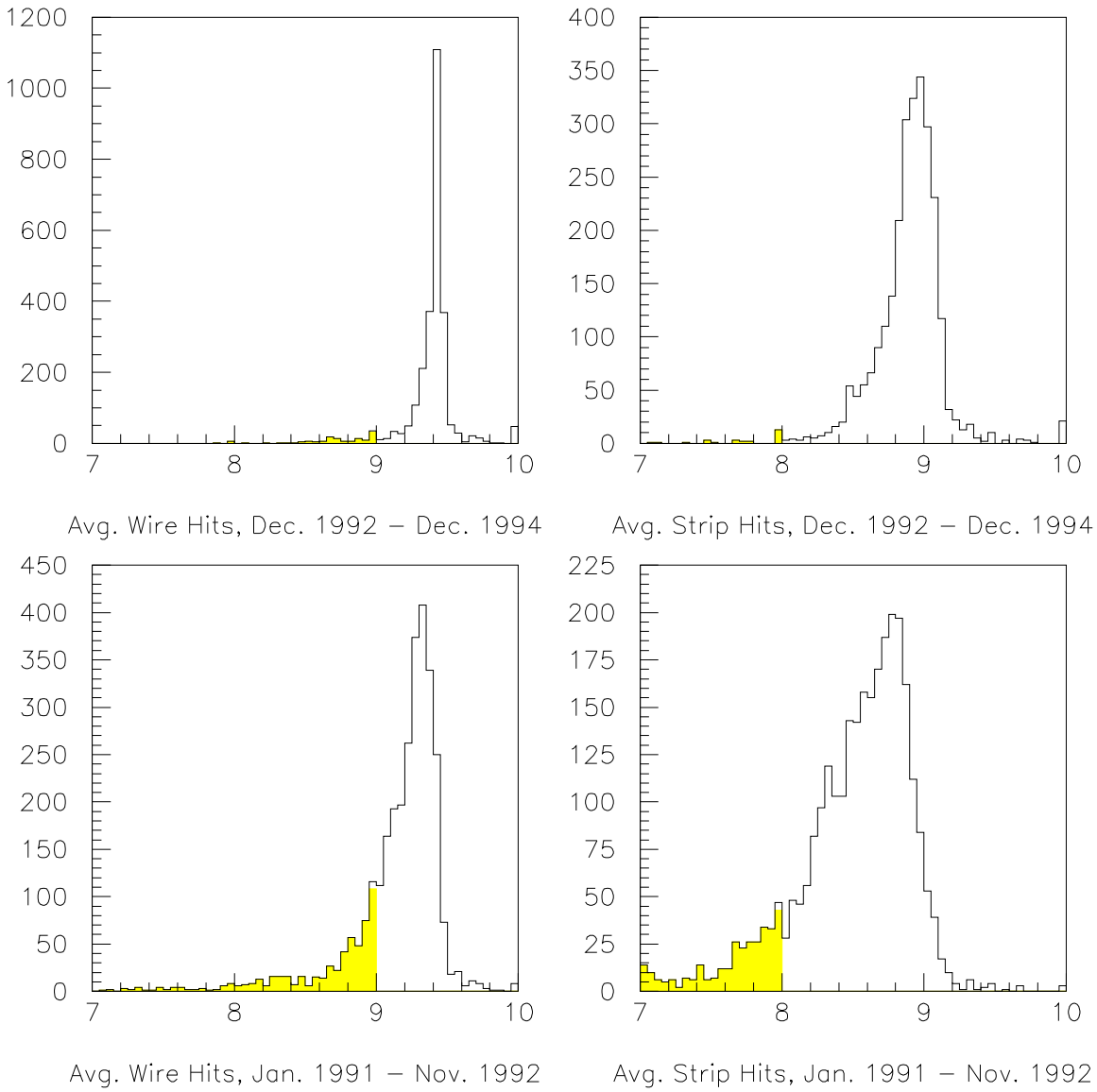

Figure 1: Distributions of the average number of planes of strips and wires hit by run for ten-plane crossing muons, shown for post- and pre-Dec. 1992 data. Shaded areas indicate the runs that were cut.

To further insure the quality of the dataset, cuts were placed on the inclusion of data from a μVAX for a whole data run, after the event cuts described above were applied. The unit of a μVAX was used because data acquisition problems usually

show up at the μVAX level. To eliminate any overall detector dead time or noise problems, a gaussian fit to the muon rates per run for each supermodule (SM) was performed. All data from a μVAX for a given run was discarded if the data rate for one of its two component supermodules had a rate more than three sigma above or below the mean of this fit during that run. Furthermore, the average number of wires and strips which fired during a run for ten plane crossing muons must be above the minimum values of 9.0 for wires and 8.0 for strips, as shown in Figure 1. This cut was again calculated for each SM and applied to the data from the whole μVAX. The efficiency cut avoided any overall streamer tube efficiency problems and affected runs before December 1992 the most, because the streamer tube system was not fully optimized until this point. The fractions of the total data lost to each cut are shown in Table 1.

	Cut	% of total data lost	
		May 1991-Nov 1992	Dec 1992-Dec 1994
Event Cuts	Only 10-plane crossers in a single module kept	53.5	52.9
	Only Single Muons	4.46	4.51
	Total event cuts, %muons	57.9	57.4
Run Cuts	All six SM not active	37.6	12.1
	Efficiency cuts (Figure 1)	27.3	6.78
	μ rate on a SM is more than 3σ from the mean	0.94	1.93
	Months cut by hand due to overall streamer tube system problems.	1.28	4.52
	Total run cuts, %livetime	67.12	25.33

Table 1: Data cuts, in % of total muons cut for Event Cuts, and % of livetime cut for Run Cuts.

After all these cuts, a total of 5.3 million muons remained over a live time of almost 44,000 μVAX-hours. The unit of μVAX-hours for livetime was used since one or more μVAXen might have failed a cut for a given run, with the rest of the detector's data remaining in the analysis. These numbers are shown in detail in Table 2, divided into two data sets: before and after the optimization of the streamer tubes.

Data set	# of Muons	Live μVAX Hours
Jan. 1992-Nov. 1992	1,545,332	12,605.9
Dec. 1992-Dec. 1994	3,778,167	31,236.9
Totals	5,323,499	43,842.8

Table 2: Data used for the Seasonal Variations analysis.

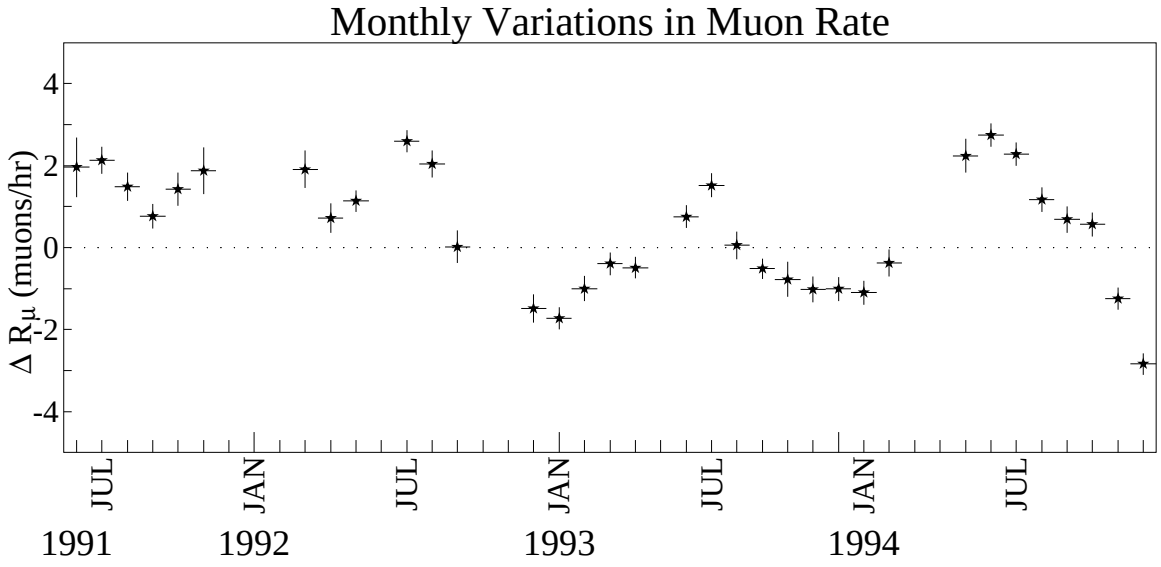

Figure 2: Monthly variations in the mean monthly rate, $\Delta R_\mu = (R_\mu - \overline{R}_\mu)$. R_μ is the mean monthly rate and R_μ = 121.6 μ/h/μVAX is the mean rate computed for the December 1992-1994 data set. The errors are dominated by statistical errors on the rates.

Figure 2 shows the ΔR_μ's calculated from the above data as a function of month. Since the data from the first two years is incomplete in the same way (the low rate winter months are missing), the $\overline{R}_\mu$ used to determine these ΔR_μ's is calculated from the last two years only, to avoid biasing $\overline{R}_\mu$ towards the high side. The resulting $\overline{R}_\mu$ is 121.6 μ/hr/μVAX.

5.5 The Temperature Data

The temperature data used in this analysis were provided by the Ispettorato Telecomunicazioni ed Assistenza Volo dell'Aeronautica Italiana. Temperatures were obtained at different atmospheric depths via weather balloon. During 1991 through 1993, four balloon flights daily were at 0h, 6h, 12h, and 18h. Temperatures were taken at eight atmospheric depths: 700 g/cm^2, 500 g/cm^2, 300 g/cm^2, 150 g/cm^2, 70 g/cm^2, 45 g/cm^2, 35 g/cm^2, and 25 g/cm^2. The data taking changed in 1994 when only two flights were flown per day, at 11h and 23h. Temperatures were available with a much finer depth sampling. However for consistency with the earlier data only data from above 700 g/cm^2 were used.

These data were used to compute a T_{eff} for each flight from Equation 21. A global T_{eff} for each month was computed by taking the simple mean of all the T_{eff} measurements obtained in each month. The errors on these data points are the standard deviations of these measurements in each month. $\overline{T}_{eff}$, the mean of these means, was 217.8 °K. Figure 3 shows the fluctuations of each month about this mean. The points in 1994 have larger error bars than the rest, probobly due to the limits of

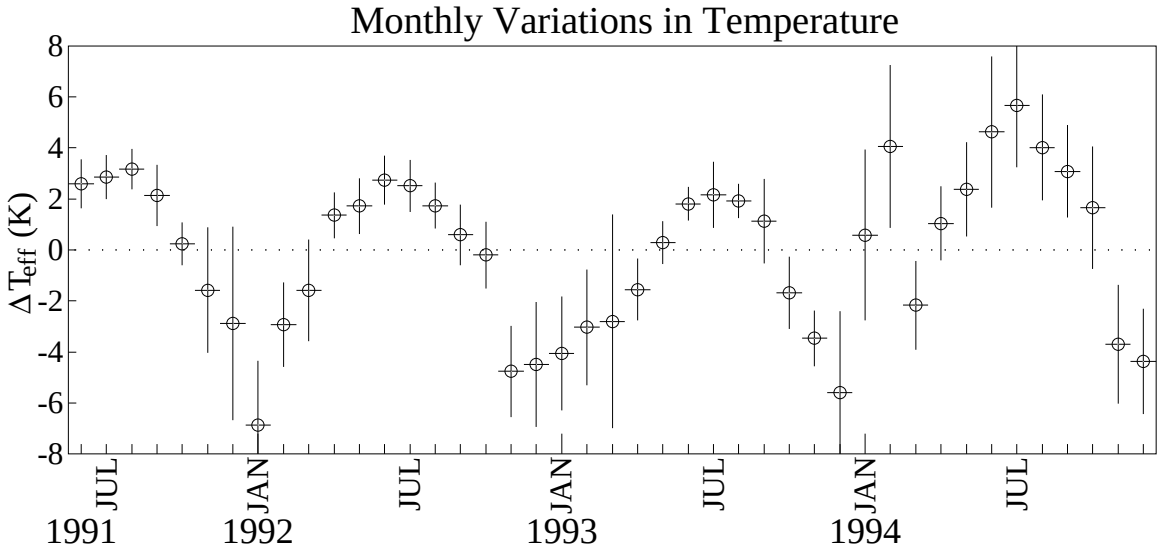

Figure 3: Monthly variations in the effective temperature, $\Delta T_{eff} = (T_{eff} - \overline{T}_{eff})$, where T_{eff} is the mean of the monthly effective temperature distribution and $\overline{T}_{eff} = 217.8°K$ is the mean effective temperature for the whole data set (1991-1994). The errors on the fluctuations are taken as the standard deviation in the T_{eff} distribution for that month.

twice-daily balloon flights during that year.

5.6 The Temperature / Rate Correlation

An overlay between the rate and temperature fluctuations for the data from December 1992 onward (Figure 4) shows a clear correlation between these two distributions. Since the rate data is incomplete and MACRO was not optimized for data taking before December 1992, this analysis is primarily of the data from the optimized period of this date onwards.

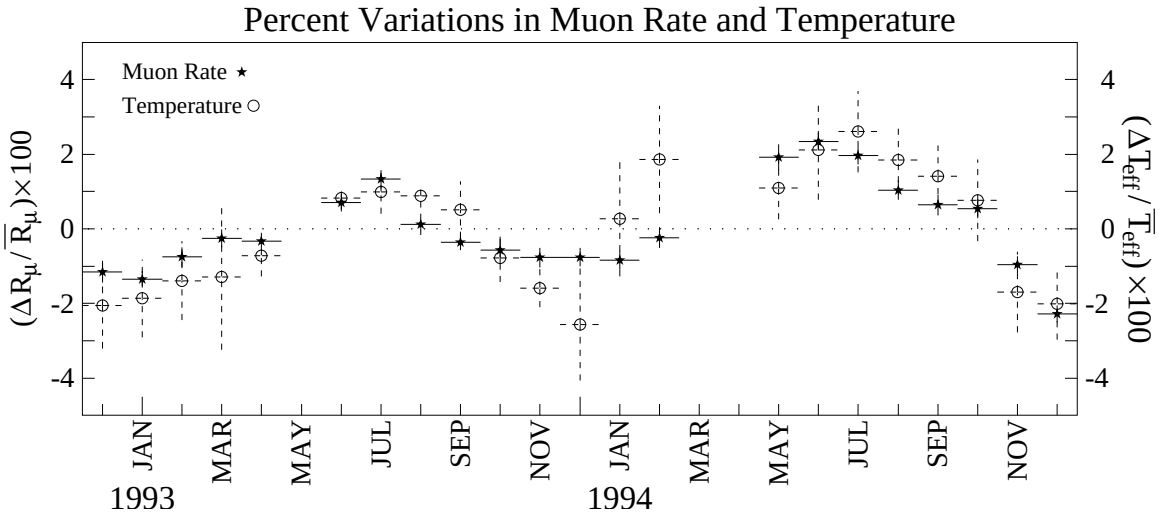

Figure 4: The superposition of the mean monthly variations in the muon rate, $\Delta R_\mu / \overline{R}_\mu(\%)$, and the mean monthly variations in the effective temperature, $\Delta T_{eff} / \overline{T}_{eff}(\%)$ for the December 1992-1994 data set.

To quantify the correlation seen in Figure 4, the correlation coefficient has been computed. The chance of the null hypothesis -- that is, the chance of random fluctuations producing such a correlation -- has also been computed. These numbers are shown in Table 3 on page 88 and show quantitatively that the two sets of fluctuations are highly correlated.

This analysis has been repeated for all the data. To do so, the rate and temperature fluctuations were binned by month over all four years. The results of this procedure are shown graphically in Figure 5, and the correlation parameters are also listed in Table 3. These data are also highly correlated, although slightly less so than the two year average, due to the inclusion of the incomplete data from 1991 and 1992.

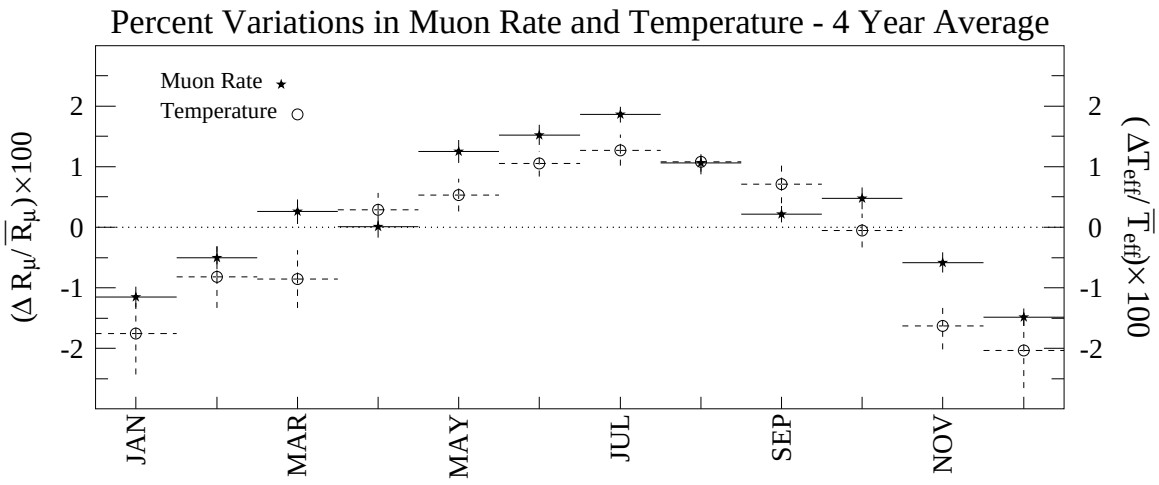

Figure 5: The superposition of the mean monthly variations in the muon rate, $\Delta R_\mu/\overline{R}_\mu(\%)$, and the mean monthly variations in the effective temperature, $\Delta T_{eff}/\overline{T}_{eff}(\%)$ for the averaged total data set.

5.7 Experimental Determination of α_T for muons at MACRO

In determining α_T, the data from December 1992 through December 1994 was first taken alone, as described above. Each month's pair of $\Delta R_\mu/\overline{R}_\mu$ and $\Delta T_{eff}/\overline{T}_{eff}$ points were input to a straight line fitting algorithm, to uncover the slope in the relation given in Equation 13. Since both coordinates in this fit have associated errors, a simple least squares fit cannot be used. An algorithm capable of dealing with two sets of errors (given in **Numerical Recipes**[18]) was used to compute $\alpha_T = 0.83 \pm 0.13$, as shown in Table 3. Repeating this analysis with all four years of data yields $\alpha_T = 0.98 \pm 0.12$.

Dataset	Correlation Coefficient	Prob. of Null Hypothesis	α_T
1993-1994	0.83	1.70e-06	0.83 ± 0.13
1991-1994	0.91	3.30e-05	0.98 ± 0.12

Table 3: Correlation Coefficient and Probability that ΔR_μ and ΔT_{eff} are uncorrelated (Null Hypothesis).

5.8 The Predicted α_T for MACRO

To match the assumption of meson energies in the scaling limit made in Section 5.3, the calculation of the expected α_T was performed with the assumption that the muons seen at MACRO come only from pion decay.

Barrett has shown[2] that for a spectrum of the type described in Equation 2, Equation 22 becomes

$$\alpha_T = -\frac{E_{th}}{I_\mu^0}\frac{\partial I_\mu}{\partial E_{th}} - \gamma \ . \qquad \textbf{(23)}$$

Evaluating this expression using Equation 2 yields

$$(\alpha_T)_\pi = 1 \Big/ \left[1 + \frac{\gamma}{(\gamma+1)} \times \frac{\epsilon_\pi}{1.1 E_{th}\cos\theta}\right] \qquad \textbf{(24)}$$

for the temperature decay coefficient due to pion decay alone.

The average of this equation,

$$<\alpha_T>_\pi = \left\langle 1 \Big/ \left[1 + \frac{\gamma}{(\gamma+1)} \times \frac{\epsilon_\pi}{1.1 E_{th} \cos\theta} \right] \right\rangle , \qquad \textbf{(25)}$$

has been computed via Monte Carlo. This is not the Monte Carlo described in Chapter 3, but rather a special purpose program. In Equation 25, $\gamma = 1.78$, the spectral index of the muon intensity at MACRO[19]; $\epsilon_\pi = 115$ GeV, is the pion critical energy; $E_{th}\cos\theta$ is the product of the threshold energy and cosine zenith angle for each muon involved, which is the term computed by Monte Carlo.

In the Monte Carlo calculation, a muon energy and zenith angle are chosen from MACRO's known muon intensity distribution[19]. A random azimuthal angle is chosen. Given this zenith and azimuthal angle, the rock depth in this direction is selected from a table of the known rock distribution above MACRO. A rock depth can be equated with a threshold energy by Equation 4. The chance that the muon would not penetrate to MACRO is selected from the MACRO survival probability tables. If the muon were to reach MACRO, it is placed upon the detector at a random location and the geometry is calculated to see if it would cross ten planes of streamer tubes in a single module of the lower detector. This criterion is applied to match that required for the real data.

One more cut on the simulated muons is needed. The real data are restricted to single muons. However, the input spectrum used in this Monte Carlo includes all muons. This final cut excludes muons from the simulation which would have been

seen by MACRO as double muons. This effect should be small, given the small (less than 5%) fraction of double muons appearing in MACRO's data, but it could bias the result because double muons come from parents of higher energy. Should the effect of double muons be small, the effects of triple and higher multiplicity muons can be neglected, due to their even more rare nature.

To decide if a simulated muon would be seen by MACRO as a double, a primary energy is selected for each muon which meets all the other cuts. This energy is selected from the muon response curve computed by Gaisser[20], extrapolated to the energy chosen for the muon. This extrapolation assumes that the response curve scales with energy[21]. A composition for this simulated primary is selected using the "Sigma" spectrum. This mass spectrum is the best fit to MACRO's multiple muon data[22], and is a combination of the proton and helium spectra from JACEE[23] with the heavier nucleon spectrum from CRN[24]. The muon yield of a primary of the energy selected is then calculated using the parameterizations given by Gaisser[6]. Although this yield is computed for a minimum muon energy, calculations show that the ratio of the median energy of parent nucleons to minimum muon energy falls with increasing energy. Thus, the selection of a minimum muon energy errs on the side of a larger effect on α_T from double muons. Therefore, if this effect, including this assumption, is shown to be small, then the actual effect will be even smaller.

If the simulated primary results in the observed muon being part of a double muon, then the second muon in the pair is placed on MACRO. The distance of the second muon from the first is selected from the lateral spread distribution obtained

from the same parameterizations as gave the multiplicity, and the direction is a random rotational angle. If this second muon would also hit MACRO, this simulated muon is cut.

The product $E_{th}\cos\theta$ is calculated from the simulated muons that pass all these cuts. This value is input to Equation 25, and an expected $<\alpha_T>_\pi$ calculated. The result is $<\alpha_T>_\pi = 0.96$.

5.9 The Kaon Contribution

The muons seen in MACRO come from decays of both π and K mesons. The assumption of pions only was made in Section 5.3, to use the simplifications provided by being in the scaling limit energy regime, where interactions dominate. However, the calculation based upon Equation 2 suggests that 23% of the muons recorded by MACRO come from kaon parents. How does this affect the calculated α_T?

The sensitivity of the muon intensity to atmospheric intensity varies with the relative importance of the interaction and decay processes in the pion and kaon cascades that are the parents of the muons observed by MACRO. When interactions dominate, temperature fluctuations translate directly into muon rate fluctuations, since the density of the interacting medium (the atmosphere) is related to temperature. When decays dominate, the muon rate is less sensitive to temperature changes, because the muons are being produced via decays regardless of the state of the atmosphere. The "critical energy" separates these two regimes. If $m_\pi c^2$ is the rest energy of a pion, $c\tau_\pi$ is the distance traversed by a relativistic pion in its mean

lifetime, and $H(T) = RT/Mg$ is the atmospheric scale height for an isothermal, exponential atmosphere, then interactions dominate when

$$E_\mu \gg \epsilon_\pi = \frac{m_\pi c^2 H(T)}{c\tau_\pi} \ , \qquad \textbf{(26)}$$

because most interactions occur in the first few interaction lengths. A similar expression holds for kaons.

While the muons seen at MACRO come from meson parents of energies much greater than the pion critical energy, their energies are not always much greater than the kaon critical energy. Thus the scaling limit assumption for kaons is not valid. However, if we naively make this assumption anyway, a lower limit to the magnitude of the effect of kaons upon α_T can be calculated. Since kaons have a much shorter decay length than pions, kaons have the effect of decreasing α_T even in the scaling limit approximation because a larger fraction of kaons will decay rather than interact at a given energy. At MACRO's energies, α_T will be reduced even further, because even more kaons will decay than in the scaling limit. An estimate of the minimum effect that kaons can have on α_T comes from

$$\alpha_T = (\alpha_t)_\pi (1 - \zeta_K) \ , \qquad \textbf{(27)}$$

where ζ_K is the kaon correction to α_T in the scaling limit. Changes to Λ from Equation 19 introduced by this approximation have a negligible effect on the value of

T_{eff}, since Λ_K differs from Λ_π by less than 15%[6]. This means that we can test our determination of α_T using the T_{eff} from Equation 20 against the hypothesis that $\zeta_K = 0$.

Computing $<\alpha_T>$ by the means described in Section 5.8, under the assumption that the scaling limit is valid for kaons, we find $<\alpha_T> = 0.90$, or a value for ζ_K of 0.06. The experimental value for α_T from the clean 1993-1994 data set given in Table 3 is below even this $<\alpha_T>$, which is consistent with the presence of kaons. Unfortunately, the size of the error on this value is too large to allow a significant statement to be made regarding the presence of kaon parents for MACRO's muons. The magnitude of this error is not entirely due to lack of statistics on the muon rates, but primarily to the uncertainties in the average ΔT_{eff} for each month. The actual temperature of the upper atmosphere varies significantly on the time scale of a month. This creates error bars on ΔT_{eff} too large to allow the determination of α_T to the precision necessary to make a statistically significant statement about the kaon parents. The kaon component is a minimum of a 6% effect on top of a 4% fluctuation, a very small effect.

5.10 Conclusions

The measured α_T given in Table 3 agrees with the calculated $<\alpha_T>_\pi$ of 0.96 within errors for both methods of grouping the data. It is unlikely these correlations are due to random fluctuations in the data. Therefore, MACRO is sensitive to the seasonal variations in the absolute muon flux, a peak-to-peak effect of only several

percent. Additionally, the measured α_T is consistent with the presence of kaon parents of the observed muons, although this presence cannot be claimed with high statistical significance.

Figure 6 shows this result in comparison the other underground experiments referenced in Section 5.1. These experiments give their results in the common historical unit of %/°K. These units were converted to the units used in this analysis for $<\alpha_T>_\pi$ using the T_{eff} used in the respective analyses. The curve is the expected value of $<\alpha_T>_\pi$ as a function of depth (and thus, of energy). It is calculated for muons from pion decays only, with a correction for low energy muons decaying into electrons[2]. At low energies, $<\alpha_T>_\pi$ is small because the cascades are dominated by decays and the effect of changing air density is unimportant to the decay of the parent mesons. Because the cascades are dominated by collisions and the cross sections for these collisions do not depend strongly on energy, $<\alpha_T>_\pi$ increases slowly at high energies.

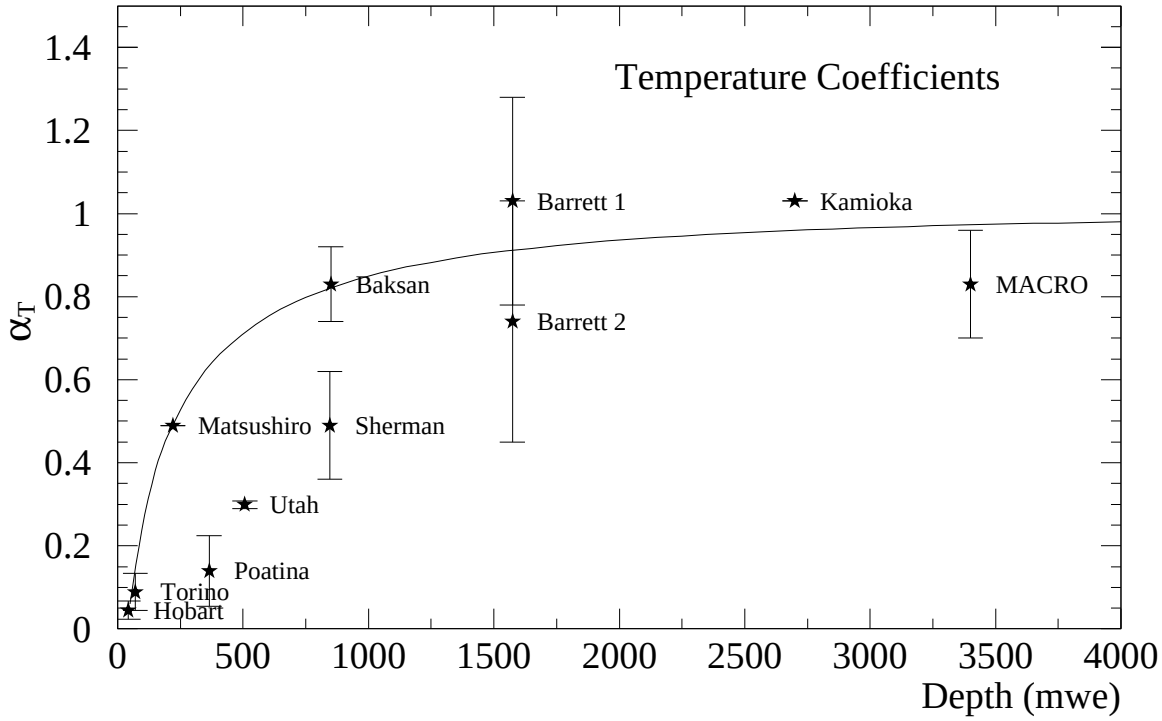

Figure 6: Experimental determination of $<\alpha_T>_\pi$. This analysis is the "MACRO" point. The other points are the experiments referenced in Section 5.1.

References

1. Ambrosio, M. *et al.*, 1996, The MACRO Collaboration, "Seasonal Variations in the Underground Muon Intensity as Seen by MACRO", preprint.

2. Barrett, P., Bollinger, C., Cocconi, G., Eisenberg, Y., and Greisen, K., 1952, "Interpretation of Cosmic-Ray Measurements Far Underground", *Rev. Mod. Phys.* **24**, 133.

3. Duperier, A., 1949, "The Meson Intensity at the Surface of the Earth and the Temperature at the Production Level", *Proc. Phys. Soc. A* **62**, 684.

4. Duperier, A., 1951, "On the Positive Temperature Effect of the Upper Atmosphere and the Process of Meson Production", *J. Atmos. Terr. Phys.* **1**, 296.

5. Trefall, H., 1955, "On the Positive Temperature Effect in the Cosmic Radiation", *Proc. Phys. Soc. A* **68**, 625.

6. Gaisser, T., 1990, **Cosmic Rays and Particle Physics**, Cambridge University Press, Cambridge, Chapter 6.

7. Sagisaka, S., 1986, "Atmospheric Effects on Cosmic-Ray Muon Intensities at Deep Underground Depths", *Il Nuovo Cimento C* **9**, 809.

8. Barrett, P., Cocconi, G., Eisenberg, Y., and Greisen, K., 1954, "Atmospheric Temperature Effects for Mesons Far Underground", *Phys. Rev.* **95**, 1573.

9. Cini-Castagnoli, G., and Dodero, M.A., 1967, "Temperature Effect of the Muon Component Underground and Pion Attenuation Lengths", *Il Nuovo Cimento B* **51**, 525.

10. Humble, J.E. *et al.*, The Poatino Group, 1979, "Variations in Atmospheric Coefficients for Underground Cosmic Ray Detectors", *Proc. 16th ICRC (Kyoto)* **4**, 258.

11. Cutler, D.J. *et al.*, The Utah Group, 1981, "Meteorological Effects in Cosmic Ray Productions", *Proc. 17th ICRC (Paris)* **4**, 290.

12. Andreyev, Yu.M *et al.*, The Baksan Collaboration, 1991, "Season Behavior of the Diurnal Intensity of Muons with $E_\mu > 220$ GeV", *Proc. 22nd. ICRC (Dublin)* **3**, 693 and references therein.

13. Murakata, K., Yasue, S., and Mori, S., 1988, "The Atmospheric Temperature Effect on the Diurnal Variation of Cosmic Ray Muon Intensity Observed at 220m Underground at Matsushiro", *J. Geoma. Geoelec.* **40**, 1023.

14. Oyama, Y. *et al.*, The Matsushiro and Kamiokande-II Collaborations, 1991, "Time Variation of the Cosmic Ray Muon Flux in Underground Detectors", *Proc. 22nd ICRC (Dublin)* **3**, 671.

15. Sherman, N., 1954, "Atmospheric Temperature Effect for μ Mesons Observed at a Depth of 846 m.w.e.", *Phys. Rev.* **93**, 208.

16. Fenton, A.G., Jacklyn, R.M., Taylor, R.B., 1961, "Cosmic Ray Observations at 42 m w.e. Underground at Hobart, Tasmania", *Il Nuovo Cimento B* **22**, 285.

17. Dorman, L.I., 1957, **Cosmic Ray Variations**, State Publishing House for Technical and Theoretical Literature, Moscow. Translation 1958 by USAF Tech. Doc. Liaison Office, WPAFB, Dayton OH.

18. Press, W.H., Teukolsky, S.A., Vettering, W.T., and Flannery, B.P., 1992, **Numerical Recipes in Fortran**, 2nd edition, Cambridge University Press, Cambridge.

19. Ambrosio, M. *et al.*, The MACRO Collaboration, 1995, "Vertical Muon Intensity Measured with MACRO", *Phys. Rev. D* **52**, 3793.

20. Gaisser, T.K., 1974, "Calculation of Muon Yields, Response Functions, and Sea Level Integral Energy Spectrum Using Recent Accelerator Data and Feynman Scaling", *J. Geophysical Research* **79**, 2281.

21. Gaisser, T.K., private communication, May 1996.

22. Ahlen, S. *et al.*, The MACRO Collaboration, and Aglietta, M. et al, the EASTOP Collaboration, 1994, "Study of the Primary Cosmic Ray Composition Around the Knee of the Energy Spectrum", *Phys. Lett. B* **337**, 376.

23. Burnett, T.H. *et al.*, The JACEE Collaboration, 1990, "Energy Spectra of Cosmic Rays Above 1 TeV per Nucleon", *Ap. J. Lett.* **349**, L25.

24. Muller, D. *et al.*, The CRN Collaboration, 1991, "Energy Spectra and Composition of Primary Cosmic Rays", *Ap. J.* **374**, 356.